



**Mean-field game approach to epidemic propagation on networks**Louis Bremaud <sup>1</sup>, Olivier Giraud <sup>1,2,3</sup> and Denis Ullmo <sup>1</sup><sup>1</sup>Université Paris-Saclay, CNRS, *LPTMS*, 91405 Orsay, France<sup>2</sup>*MajuLab*, CNRS-UCA-SU-NUS-NTU International Joint Research Laboratory, 17543 Singapore, Singapore<sup>3</sup>*Centre for Quantum Technologies*, National University of Singapore, 17543 Singapore, Singapore

(Received 24 January 2025; accepted 18 September 2025; published 3 November 2025)

We investigate an SIR model of epidemic propagation on networks in the context of mean-field games. In a real epidemic, individuals adjust their behavior depending on the epidemic level and the impact it might have on them in the future. These individual behaviors, in turn, affect the epidemic dynamics. Mean-field games are a framework in which these retroaction effects can be captured. We derive dynamical equations for the epidemic quantities in terms of individual contact rates, and via mean-field approximations, we obtain the Nash equilibrium associated with the minimization of a certain cost function. We first consider homogeneous networks, where all individuals have the same number of neighbors, and discuss how the individual behaviors are modified when that number is varied. We then investigate the case of a realistic heterogeneous network based on real data from a social contact network. Our results allow us to assess the potential of such an approach for epidemic mitigation in real-world implementations.

DOI: [10.1103/mys6-fznc](https://doi.org/10.1103/mys6-fznc)

**Introduction.** The lack of integration of dynamic human behavior into epidemic modeling remains a major limitation of contemporary epidemiological models [1–3]. Indeed, individual behavior creates a time-dependent feedback on the transmission rate that is often out of reach for epidemiologists. Relevant human behavioral dynamics can be separated into two primary categories. The first corresponds to behaviors independent of epidemics, driven by routine patterns such as day/night cycles, weekdays versus weekends, holidays, and other habitual activities. The second category includes adaptive responses triggered by the epidemic itself, where individuals adopt precautionary behaviors such as using masks, avoiding handshakes, or reducing contact to lower infection risks [4]. These adaptive behaviors may arise spontaneously or be prompted by specific nonpharmaceutical interventions, creating a feedback loop that can significantly influence the epidemic’s trajectory. Despite evidence of its importance [5,6], particularly highlighted by the COVID-19 pandemic [7], this “human-in-the-loop” factor is often not considered in predictive models, where the dynamics of human behavior is treated instead as an external parameter [2,8] acting on the transmission rate.

To address this limitation, theoretical approaches have been developed, including models that incorporate parallel information spread [9,10] or utilize payoff-based frameworks (see Poletti *et al.* [11], or more recently, Amaral *et al.* [12]). In this study, we will focus on a recent and impactful approach: the mean-field game (MFG) paradigm. In short, MFGs are tools derived from game theory that enable us to incorporate strategic interactions within systems involving a large number of agents. This game-theoretic framework makes it possible to account for anticipation effects arising from individuals optimizing intertemporal costs, and to describe “free-rider” behaviors, where individual optimization deviates from the collective societal optimum [4]. The solution associated with

the MFG is referred to as a Nash equilibrium, meaning that no individual would benefit from modifying her strategy—that is, her behavior over the course of the epidemic—if the strategies of others remain unchanged. For a comprehensive mathematical introduction to MFG, see [13], and for applications of MFG to epidemiological modeling, see [14] and [8] for a recent review.

In this Letter, we consider the propagation of an epidemic where contacts between individuals can be described by a network. In such an instance, the structure of the underlying contact network, including factors such as contact heterogeneity, correlations, clustering, and other forms of network organization, has been demonstrated to have an important influence on epidemic dynamics [15–20]. For instance, heterogeneity is known to significantly reduce the epidemic threshold on networks and to increase the propagation of the virus compared to a homogeneous network of the same average degree [17,21]. Correlations between degrees, reflected by the assortativity [22] of the network and the clustering level [23], have also been shown to play a significant role in the propagation of epidemics.

On top of this network structure, we implement an MFG framework. In the MFG approach, individuals are grouped into relevant classes to facilitate a mean-field treatment, requiring the identification of key factors driving individual behavioral responses. For instance, in [24], the age-based social structure is considered, along with the contact location (e.g., schools, households, workplaces), recognizing that age significantly influences the risk of infection in many diseases, while different locations lead to distinct contact patterns. For epidemics on networks, we will make the basic assumption that individuals with the same number of neighbors behave in the same way.

The objective of this paper is to examine how individuals’ spontaneous behavioral responses are shaped by network

structure within a susceptible-infected-recovered (SIR) model on networks. We begin by presenting a model that is grounded in the MFG approach. We then analyze the impact of network degree by examining Nash equilibrium outcomes on homogeneous networks. Finally, we demonstrate how heterogeneity and network correlations give rise to specific effects on realistic networks.

*The MFG framework on networks.* We consider a population of  $N$  individuals ( $N$  large), represented by nodes of a network. The possible contacts of an individual are the neighboring nodes on the network. The number of these contacts is called the degree of the individual, denoted  $k$ . The degree distribution is denoted by  $P(k)$ , and the two-point degree correlation matrix is represented by  $G_{kk'} = P(k'|k)$ , which is the conditional probability, for a given node of degree  $k$ , to have a neighbor of degree  $k'$ . Here, we consider Markovian networks, defined by the fact that they are fully characterized by  $P(k)$  and  $G_{kk'}$  [25].

Each individual, or node of the network, can be in one of three possible states  $x = s, i, r$  for, respectively, susceptible, infected, and recovered. Contamination occurs via edges connecting a susceptible individual to an (asymptomatic) infected individual. The dynamics follows a standard Markov process: during the time interval  $[t, t + dt]$ , an edge between a susceptible and an infected individual transmits the disease with probability  $\lambda(t)dt$ . As in the basic SIR model, infected individuals recover from the disease during that time interval with probability  $\gamma dt$ . In view of the mean-field treatment of the problem, we assume that nodes of a given degree and state are equivalent, which allows us to characterize the dynamics by the average quantities  $S_k, I_k, R_k$ , giving the relative proportion of individuals of degree  $k$  in the state susceptible, infected, or recovered at time  $t$ . Moreover, we make the degree pairwise approximation [26,27], which posits that only correlations of degree and state between nearest neighbors on the network play a role in the dynamics. We thus introduce the conditional probability  $G_{kk'}^{xy}$  for a given node to be of state  $y$  and degree  $k'$ , knowing that this node has a neighbor of state  $x$  and degree  $k$ , a quantity which accounts for all pairwise correlations inside the network.

On top of the above SIR model, we implement an MFG setting in which individuals control their own contact rate via a control variable  $n(t)$  which they can adjust. We assume that the transmission rate between individuals  $a$  and  $b$  is symmetric and given by  $\lambda^{(0)}n_a(t)n_b(t)$ , where  $\lambda^{(0)}$  represents the baseline rate in the absence of any control. As in [24], we assume that contamination occurs through (a vanishingly small proportion of) asymptomatic infected individuals, as symptomatic ones would isolate themselves after becoming ill [28]. As these asymptomatic infected individuals share the same knowledge as those who are susceptible, they behave as susceptible (see [24] for a detailed discussion). Therefore, only the control variable of susceptible (or infected asymptomatic) individuals matters, since the others are taken out of the game. Physically,  $n_a(t)$ , which we call the “effort parameter,” represents the willingness of individual  $a$  to engage in risky interactions with her neighbors. In the absence of effort we have  $n_a(t) = 1$ , while the maximum effort corresponds to some fixed value  $n_a(t) = n_{\min}$ . In our mean-field framework, at the Nash equilibrium, the behavior of the agents only depends on

their degree  $k$ , and one defines one control variable  $n_k(t)$  for each degree. The effective transmission rate between individuals of degree  $k$  and  $k'$  is then given by  $\lambda^{(0)}n_k(t)n_{k'}(t)$ . Note that  $n_k$  is assumed to be independent of the neighbor's degree  $k'$ . While this assumption may overlook some practical circumstances, it simplifies both the analytical and numerical resolution of the model.

*Epidemic dynamics.* Considering now the dynamical equations describing our system, we introduce the following transition rates. We denote by  $T_{x \rightarrow z}^k dt$  the probability for the state  $x$  of a node of degree  $k$  to change to state  $z$  in the time interval  $dt$ , and by  $T_{(x,y) \rightarrow (x',y')}^{kk'} dt$  the probability for an edge of type  $(x, y)$  and degrees  $(k, k')$  to become of type  $(x', y')$ . As shown in the Supplemental Material [29], the only nonzero rates are

$$T_{i \rightarrow r}^k = \gamma, \quad (1a)$$

$$T_{s \rightarrow i}^k = \lambda^{(0)}n_k(t)k \sum_{k'} n_{k'}(t)G_{kk'}^{si}(t), \quad (1b)$$

$$T_{(s,x) \rightarrow (i,x)}^{kk'} \simeq \lambda^{(0)}n_k(t) \left[ n_{k'}(t)\delta_{x,i} + (k-1) \sum_{k''} n_{k''}(t)G_{kk''}^{si}(t) \right], \quad (1c)$$

where in Eq. (1c), we have used the pairwise approximation [26,27]. The two terms in Eq. (1c) reflect the fact that contamination of a susceptible node along a susceptible-infected edge can come from the infected neighbor (Kronecker delta) or from the  $(k-1)$  other neighbors of the susceptible node [30].

With these notations, the SIR system for each degree can be expressed as

$$\dot{S}_k(t) = -S_k(t)T_{s \rightarrow i}^k, \quad (2a)$$

$$\dot{I}_k(t) = S_k(t)T_{s \rightarrow i}^k - I_k(t)T_{i \rightarrow r}^k, \quad (2b)$$

$$\dot{R}_k(t) = I_k(t)T_{i \rightarrow r}^k. \quad (2c)$$

Within the pairwise approximation [26,27], that is, neglecting three-point correlations (and beyond) which should appear in its evolution, the dynamics of  $G_{kk'}^{si}$  is given (see Supplemental Material [29]) by the coupled equations

$$\begin{aligned} \frac{d}{dt}(X_k G_{kk'}^{xy}) &= \sum_{x'y'} X_k' G_{kk'}^{x'y'} T_{(x',y') \rightarrow (x,y)}^{kk'} \\ &\quad - X_k G_{kk'}^{xy} \sum_{x'y'} T_{(x,y) \rightarrow (x',y')}^{kk'}, \end{aligned} \quad (3)$$

where  $X_k$  denotes the relative proportion of agents of state  $x$  in the class  $k$ . The pairwise approximation has been shown to be very accurate on Markovian networks [31].

The system (1)–(3) forms the Kolmogorov system of our MFG. Given the set  $\mathcal{S} = \{n_k(\cdot)\}_k$  of all collective strategies of degree- $k$  individuals at all times, this system describes the evolution of all epidemic rates.

*Individual optimization.* In the MFG setting, the  $n_k(t)$  are given as the result of individual optimization of agents and depend on the epidemic rates. In order to obtain the  $n_k(t)$ , we assume that individuals of degree  $k$  are sensitive to an intertemporal mean-field cost between the time  $t$  at which the

TABLE I. Table of parameters used in our simulations.  $\lambda^{(0)} = 4/\langle k \rangle$  allows us to appropriately compare epidemics on different networks by rescaling the infection rate and keeping a constant infection probability  $\lambda^{(0)}\langle k \rangle$  on average.

$(S_0, I_0, R_0) = (0.995, 0.005, 0), \quad \gamma = 1, \quad \lambda^{(0)}\langle k \rangle = 4$
$r_I = 50, \quad n_{\min} = 0.1$

optimization is performed and the end of the game at time  $T$ . Here, we choose  $T$  large enough so that herd immunity is reached well before  $T$ . At time  $t$ , a representative *susceptible* individual  $a$  of degree  $k$  wishes to optimize the average cost [24,32]

$$\mathfrak{C}(n_a(\cdot), \mathcal{S}, t) = \int_t^T [\lambda_a(\tau) r_I + f_k(n_a(\tau))] P_a(\tau|t) d\tau, \quad (4)$$

in which we have introduced the force of infection perceived by individual  $a$ ,

$$\lambda_a(\tau) = \lambda^{(0)} n_a(\tau) k \sum_{k'} n_{k'}(\tau) G_{kk'}^{si}(\tau), \quad (5)$$

obtained in the same way as Eq. (1b), and  $P_a(\tau|t) \equiv \exp[-\int_t^\tau \lambda_a(u) du]$  the probability for individual  $a$  of still being susceptible at time  $\tau > t$ , knowing that she is susceptible at time  $t$ . In (4), the cost function is the sum of a cost  $r_I$ , incurred in case of an infection, and a social cost  $f_k$ . Here, we assume that the infection cost  $r_I$  is independent of  $k$  (all individuals are equally affected by the disease), while the social cost of being deprived of contacts is likely to depend on the degree and hence is a function of  $k$ .

From an individual's perspective, the best strategy at time  $t$  is to tune her effort parameter  $n_a(\tau), \tau > t$ , in order to minimize her own foreseeable cost (4). Introducing the value function

$$U_a(t) = \begin{cases} \min_{n_a(\cdot)} \mathfrak{C}(n_a(\cdot), \mathcal{S}, t), & a \text{ susceptible at } t \\ 0, & a \text{ infected/recovered at } t, \end{cases} \quad (6)$$

one can show, following the same reasoning as in [24], that

$$-\frac{dU_a}{dt} = \min_{n_a(t)} [\lambda_a(t)(r_I - U_a(t)) + f_k(n_a(t))]. \quad (7)$$

This is a differential equation for which the final condition  $U_a(T) = 0$  is fixed; it is known as the Hamilton-Jacobi-Bellman equation of the game. Finally, the MFG setting requires a consistency condition to be at a Nash equilibrium, namely that the optimal strategy  $n_a^*(t)$  which minimizes the right-hand side of (7) should be the same as the one entering into the Kolmogorov system of equations (1)–(3) for individuals with the same degree. For any individual  $a$  of degree  $k$  one thus has

$$n_a^*(t) = n_k(t). \quad (8)$$

Equations (1)–(3), together with Eqs. (7) and (8), form the MFG system of our game. We solve it numerically using a gradient descent approach (for details, see [33]).

For all our simulations, the parameters characterizing the epidemics are those given in Table I [34]. For the social cost

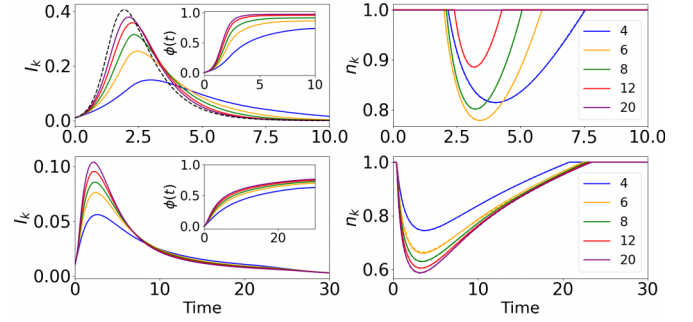


FIG. 1. Left column: Dynamics of infected individuals, corresponding to the Nash equilibrium, with the parameters of Table I for different homogeneous networks, with  $k = 4$  (blue), 6 (orange), 8 (green), 12 (red), 20 (purple), and classical SIR model (black dashed); the social cost function is  $f_k^\epsilon$  with  $\epsilon = 1$  (top) and  $\epsilon = 0$  (bottom). Inset: dynamics of the probability  $\phi(t) = 1 - P(t|0)$  to be infected before  $t$ . Right column: Dynamics of the corresponding individual effort parameter, with the same parameters and color code as for the left column.

function, we chose the specific form

$$f_k^\epsilon(n(t)) = k^\epsilon \left( \frac{1}{n(t)} - 1 \right), \quad \epsilon = 0 \text{ or } 1, \quad (9)$$

which allows us to explore different regimes of social dependence on neighbors. Physically, the choice  $\epsilon = 1$  implies that a constant social cost of  $(\frac{1}{n_a(t)} - 1)$  is assigned to each neighbor, which means that for a fixed fraction of contacts lost, an individual with a higher number of neighbors is more impacted than an individual with fewer neighbors. In the case  $\epsilon = 0$ , the social cost is the same for all individuals, whatever their degree.

**Homogeneous networks.** We first consider the simplest case of homogeneous networks (or regular graphs), where each node has the same number  $k$  of neighbors. After numerically solving the system of equations discussed above and reaching a Nash equilibrium, we obtain the epidemic rates and associated effort parameters. They are displayed in Fig. 1 for the two different possibilities  $f_k^{0,1}$  (note that here  $\epsilon = 0$  or 1 only affects the relative importance of the social cost with respect to the infection cost). Several observations can be made.

First, we observe in Fig. 1 that while individuals reduce their contact rate predominantly during the epidemic peak, their maximal effort occurs slightly after the peak is reached (see, for instance, the case  $k = 4$  on the first row), and they maintain their effort well beyond the peak. This suggests that individuals engage in a form of “reverse anticipation.” More precisely, it is not the anticipation of the incoming epidemic that motivates their behavior, but the compound effect of the actual (present time) intensity of the epidemic and of the *anticipation of its end*. Indeed, at the onset of the epidemic, the prospect of maintaining a significant effort for the whole duration of the epidemic, while the latter is still growing slowly and individuals anticipate that collective immunity will not be reached anytime soon, appears more costly (with our choice of parameters) than paying the “one-time” cost of infection. However, as collective immunity is in sight, shortly before the epidemic peak and for some time after, it becomes

advantageous to make efforts to avoid infection, since the epidemic is still severe, and the remaining time before the epidemic is over is reasonably short. It then becomes advantageous for susceptible individuals to make significant efforts, as they have a good chance of avoiding infection forever if they protect themselves for a relatively short period.

While the mechanism described above is rather generic, the precise range and intensity at which it is at play, of course, depends on the choice of parameters. In particular, epidemics on random homogeneous networks progress faster and are more intense as  $k$  increases [32]. For constant  $f_k$  ( $\epsilon = 0$ , second row of Fig. 1), the ratios between social effort and infection cost remain essentially constant across degrees, and are fairly low for our choice of parameters. This leads to effort patterns that are similar across degrees, with individuals tending to protect themselves by “flattening” the infection curve  $\phi(t)$ , thereby minimizing their probability of infection. The only difference between classes is that networks in which individuals have a higher degree face more intense epidemics, requiring greater and more prolonged effort while maintaining the same overall pattern. On the other hand, when the social cost  $f_k$  increases with  $k$  ( $\epsilon = 1$ , first row of Fig. 1), this increasing social cost may compete with the one of the infection. As Fig. 1 shows, these two factors essentially balance each other around a critical value  $k^* \simeq 6$ , leading to a significant intensity of effort. However, below this threshold, the epidemic is not sufficiently virulent, and above  $k^*$  efforts become too costly to justify a strong reduction of social contact. As  $k \rightarrow \infty$ , individual behavior converges to the effortless parameter  $n(t) = 1$ , and the infection curve approaches that of the classical SIR model (see dashed curve in Fig. 1).

**Heterogeneous networks** We now investigate the more realistic case of a heterogeneous network. The SIR model on such networks is usually studied by considering a scale-free distribution  $P(k)$  [21]. As the correlation matrix  $G_{kk'}$  plays a crucial role in the MFG equations, we choose to investigate a realistic network constructed in the following way: We build  $P(k)$  based on the work of Eubank *et al.* [35] and Béraud *et al.* [36]. We define it as a piecewise power-law distribution  $P(k) \propto k^{\eta(k)}$  with  $\eta(k) = 1$  for  $k \in [2, 5]$ ,  $-1.5$  for  $k \in [5, 10]$ ,  $-3$  for  $k \in [10, 100]$ , which gives a maximum of around five contacts per day. We chose the above exponents  $\eta(k)$  and intervals for  $k$  in such a way that the range of  $k$ , average, standard deviation, and maximum of that distribution are consistent with [36]. In order to perform the numerical simulations in a reasonable time, we split our distribution  $P(k)$  into batches containing approximately the same number of nodes. Namely, we consider that all nodes with degree  $k \in [\tilde{k}_i, \tilde{k}_{i+1}]$  can be treated as nodes with degree  $K_i$ , with  $K_i$  the average degree of the nodes in that interval. Our choice for the batches is given in Table II. The quality of this approximation is demonstrated in Sec. II of the Supplemental Material [29].

For a given correlation matrix  $G_{kk'}$ , one can introduce an assortativity coefficient  $r \in [-1, 1]$ , defined precisely in [22]. A positive  $r$  intuitively means that high-degree individuals will tend to have contacts with high-degree individuals, and similarly for low-degree individuals. Social contact networks are known to be assortative, and here we choose  $r$  approximately equal to 0.3, compatible with the kind of networks described in [22]. Using the Newman rewiring algorithm [37],

TABLE II. Parameters characterizing the realistic heterogeneous network used for Fig. 2: the five batches  $[\tilde{k}_i, \tilde{k}_{i+1}]$ , the average degree  $K_i$  of the nodes in each interval, and the corresponding degree distribution  $\tilde{P}(K)$  and correlation matrix  $G_{KK'}$ .

Intervals $[\tilde{k}_i, \tilde{k}_{i+1}] = [2, 5], [5, 7], [7, 10], [10, 19], [19, 100]$					
Average $K_i = (3.2, 5.4, 7.8, 12.5, 31.2)$					
Distribution $\tilde{P}(K) = (0.26, 0.25, 0.22, 0.20, 0.07)$					
$G_{KK'} = \begin{pmatrix} 0.76 & 0.03 & 0.04 & 0.06 & 0.11 \\ 0.02 & 0.78 & 0.04 & 0.06 & 0.10 \\ 0.02 & 0.03 & 0.79 & 0.06 & 0.10 \\ 0.02 & 0.03 & 0.04 & 0.80 & 0.11 \\ 0.03 & 0.06 & 0.07 & 0.11 & 0.72 \end{pmatrix}$					

we obtain a matrix  $G_{kk'}$  averaged over 10 networks of 20 000 nodes with  $r \simeq 0.3$ .

The dynamics of the epidemics and the associated effort parameters at the Nash equilibrium are obtained by solving Eqs. (1)–(8). We assume that  $G_{kk'}^{\text{xy}}(0) = X_k(0)G_{kk'}$ , which indicates that there is no correlation between states and degrees at time  $t = 0$ . The results are displayed in Fig. 2 for the two different choices of  $f_k^\epsilon$ . The specific impact of a realistic distribution, together with the interactions between classes (heterogeneity), can be captured. As all classes are in interaction in a heterogeneous network, we may have expected to observe a homogenization of the outcomes. We observe, on the contrary, that in all cases the spread, as a function of  $k$ , of the total number of infected at  $T$  (inset panel), increases compared to the homogeneous case.

In fact, herd immunity emerges on a global scale rather than within each degree class. High-degree nodes are infected early and cannot achieve herd immunity on their own due to their small proportion in the network. As a result, the overall virulence of the epidemic (i.e., the total number of infections at time  $T$ ) is higher for these nodes than in homogeneous networks. In contrast, low-degree nodes benefit from this dynamic: they reach herd immunity faster and with less

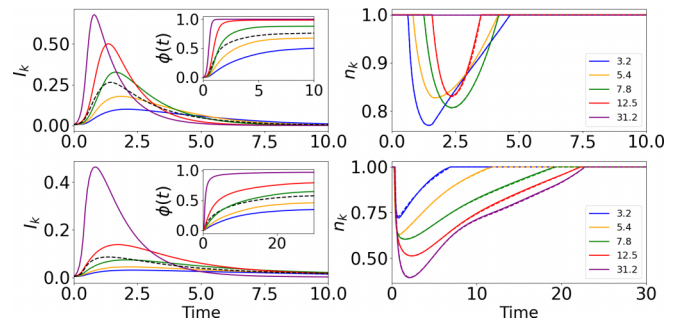


FIG. 2. Left panels: Dynamics of infected individuals at Nash equilibrium for different batches, with the parameters of Tables I and II. Inset: dynamics of the probability  $\phi(t)$  of being infected before  $t$ . Right panels: Dynamics of the corresponding individual effort parameter. Colored solid lines correspond to the dynamics (for infected and effort parameter) associated with each batch of the network:  $K = 3.2$  (blue), 5.4 (orange), 7.8 (green), 12.5 (red), 31.2 (purple). Black dashed lines represent the global proportion in the network for  $I$  and  $\phi$ . Each row represents a specific choice of  $f_k^\epsilon$ :  $\epsilon = 1, 0$  for the first and second row, respectively.



epidemic impact due to the early and widespread infection of high-degree nodes. This distinction between nodes that “benefit” or “suffer” from network heterogeneity is illustrated in Fig. 2 of the Supplemental Material [29] with an appropriate comparison.

This observation allows us to understand individual behavior in heterogeneous networks: high-degree individuals, who cannot avoid infection, have little incentive to take protective measures. In contrast, low-degree individuals benefit from avoiding infection during periods of high transmission, which motivates them to engage in early prevention efforts.

Differences in infection rates result in infection curves that strongly depend on the degree. For  $\epsilon = 1$  (Fig. 2, upper right panel), interactions between classes influence the competition between costs in a complex manner: the curve tails shorten with increasing degree, while effort levels decrease nonmonotonically. In contrast, for  $\epsilon = 0$  (Fig. 2, lower right panel), effort patterns become degree-specific in a more understandable way: high-degree individuals protect themselves, while low-degree individuals benefit from the collective immunity achieved by others more rapidly.

**Conclusion** In the present Letter, we studied the problem of epidemic propagation on networks from the point of view of mean-field games. This allowed us to analyze how individual behavior may affect the outcome of an epidemic when that behavior itself is modified at each time by the epidemic. In our model, individuals can tune the intensity of the contacts they are willing to have with others (effort parameter) in order to optimize the cost that this choice will make them incur in the future. We showed that this interplay can be described by a Hamilton-Jacobi-Bellman system of equations for the individual costs and effort parameters, coupled with a set of Kolmogorov equations describing the epidemic dynamics.

Our MFG approach to networks highlights the “reverse anticipation” effect, where individuals adjust their behavior in anticipation of the end of the epidemic—a phenomenon likely to be observed in contexts other than networks. This anticipation can be brief, as in the case of increasing social costs with  $k$ , or have a long tail, as in the case of constant social costs, when efforts effectively reduce the probability of infection without being too costly. In the homogeneous case with  $\epsilon = 1$ , the model shows a balance between the increasing social cost with  $k$  and the higher epidemic costs experienced by individuals with high degrees, while a more homogeneous behavior is observed at  $\epsilon = 0$ . The introduction of heterogeneity and assortativity in a realistic network leads to differentiated collective immunity at the node level: low-degree individuals benefit from the fast spreading of the epidemic among high-degree individuals, which reduces the effective connectivity of the remaining susceptible network. Contrary to expectations, heterogeneity reduces costs for low-degree individuals, while positive assortativity weakens this protection, as it tends to reduce heterogeneity between classes.

In both cases, the role of the social cost  $f$  on the behavior of individuals is crucial, even though the only variations of  $f$  we considered were the ones associated with its degree  $k$ . Our work underlines that a precise description of the behavior of  $f$  is a key element to go further in the practical implementation of MFG frameworks. This endeavor should benefit from the fact that the social cost properties should show little variation across epidemics, allowing large surveys to obtain the dependencies of  $f$ .

**Data availability.** The data that support the findings of this article are openly available [38]; embargo periods may apply.

- 
- [1] A. Arenas, W. Cota, J. Gómez-Gardeñes, S. Gómez, C. Granell, J. T. Matamalas, D. Soriano-Paños, and B. Steinegger, Modeling the spatiotemporal epidemic spreading of COVID-19 and the impact of mobility and social distancing interventions, *Phys. Rev. X* **10**, 041055 (2020).
  - [2] H. Salje, C. Tran Kiem, N. Lefrancq, N. Courtejoie, P. Bosetti, J. Paireau, A. Andronico, N. Hozé, J. Richet, C.-L. Dubost *et al.*, Estimating the burden of SARS-CoV-2 in France, *Science* **369**, 208 (2020).
  - [3] N. M. Ferguson, D. Laydon, G. Nedjati-Gilani, N. Imai, K. Ainslie, M. Baguelin, S. Bhatia, A. Boonyasiri, Z. Cucunubá, G. Cuomo-Dannenburg *et al.*, *Report 9: Impact of Non-pharmaceutical Interventions (NPIs) to Reduce COVID-19 Mortality and Healthcare Demand*, Vol. 16 (Imperial College, London 2020).
  - [4] P. Poletti, Human behavior in epidemic modelling, Ph.D. thesis, University of Trento, 2010.
  - [5] N. Ferguson, Capturing human behaviour, *Nature (London)* **446**, 733 (2007).
  - [6] J. M. Epstein, Modelling to contain pandemics, *Nature (London)* **460**, 687 (2009).
  - [7] B. Tang, W. Zhou, X. Wang, H. Wu, and Y. Xiao, Controlling multiple COVID-19 epidemic waves: An insight from a multi-scale model linking the behaviour change dynamics to the disease transmission dynamics, *Bull. Math. Biol.* **84**, 106 (2022).
  - [8] J. Guan, Y. Wei, Y. Zhao, and F. Chen, Modeling the transmission dynamics of COVID-19 epidemic: A systematic review, *J. Biomed. Res.* **34**, 422 (2020).
  - [9] I. Z. Kiss, J. Cassell, M. Recker, and P. L. Simon, The impact of information transmission on epidemic outbreaks, *Math. Biosci.* **225**, 1 (2010).
  - [10] X.-X. Zhan, C. Liu, G. Zhou, Z.-K. Zhang, G.-Q. Sun, J. J. Zhu, and Z. Jin, Coupling dynamics of epidemic spreading and information diffusion on complex networks, *Appl. Math. Compu.* **332**, 437 (2018).
  - [11] P. Poletti, B. Caprile, M. Ajelli, A. Pugliese, and S. Merler, Spontaneous behavioural changes in response to epidemics, *J. Theor. Biol.* **260**, 31 (2009).
  - [12] M. A. Amaral, M. M. de Oliveira, and M. A. Javarone, An epidemiological model with voluntary quarantine strategies governed by evolutionary game dynamics, *Chaos, Solitons Fractals* **143**, 110616 (2021).
  - [13] J.-M. Lasry and P.-L. Lions, Mean field games, *Jpn. J. Math.* **2**, 229 (2007).
  - [14] R. Elie, E. Hubert, and G. Turinici, Contact rate epidemic control of COVID-19: An equilibrium view, *Math. Model. Nat. Phenom.* **15**, 35 (2020).

- [15] D. J. Watts and S. H. Strogatz, Collective dynamics of ‘small-world’ networks, *Nature (London)* **393**, 440 (1998).
- [16] F. C. Santos, J. F. Rodrigues, and J. M. Pacheco, Epidemic spreading and cooperation dynamics on homogeneous small-world networks, *Phys. Rev. E* **72**, 056128 (2005).
- [17] M. Barthélemy, A. Barrat, R. Pastor-Satorras, and A. Vespignani, Dynamical patterns of epidemic outbreaks in complex heterogeneous networks, *J. Theor. Biol.* **235**, 275 (2005).
- [18] Y. Hu, L. Min, and Y. Kuang, Modeling the dynamics of epidemic spreading on homogenous and heterogeneous networks, *Applicable Analysis* **94**, 2308 (2015).
- [19] F. D. Sahneh and C. Scoglio, Epidemic spread in human networks, in *2011 50th IEEE Conference on Decision and Control and European Control Conference* (IEEE, Piscataway, NJ, 2011), pp. 3008–3013.
- [20] M. E. J. Newman, Spread of epidemic disease on networks, *Phys. Rev. E* **66**, 016128 (2002).
- [21] R. Pastor-Satorras, C. Castellano, P. Van Mieghem, and A. Vespignani, Epidemic processes in complex networks, *Rev. Mod. Phys.* **87**, 925 (2015).
- [22] M. E. J. Newman, Mixing patterns in networks, *Phys. Rev. E* **67**, 026126 (2003).
- [23] M. E. J. Newman, Random graphs with clustering, *Phys. Rev. Lett.* **103**, 058701 (2009).
- [24] L. Bremaud, O. Giraud, and D. Ullmo, Mean-field-game approach to nonpharmaceutical interventions in a social-structure model of epidemics, *Phys. Rev. E* **110**, 064301 (2024).
- [25] M. Boguñá and R. Pastor-Satorras, Epidemic spreading in correlated complex networks, *Phys. Rev. E* **66**, 047104 (2002).
- [26] P. L. Simon and I. Z. Kiss, Super compact pairwise model for SIS epidemic on heterogeneous networks, *J. Complex Netw.* **4**, 187 (2016).
- [27] M. J. Keeling, The effects of local spatial structure on epidemiological invasions, *Proc. R. Soc. London, Ser. B* **266**, 859 (1999).
- [28] We introduce the hypothesis that the number of asymptomatic individuals is vanishingly small because it simplifies the analysis without changing the mechanisms we study in any significant way. However, this assumption may need to be reconsidered when studying specific epidemics, such as the one involving the COVID-19 virus.
- [29] See Supplemental Material at <http://link.aps.org/supplemental/10.1103/mys6-fznc> for a derivation of the MFG equations and an assessment of the pairwise approximation.
- [30] Note that contamination occurs only through the fraction  $\mu I_k$  of asymptomatic individuals, with  $\mu \ll 1$ , see Eq. (2.11) of [24]; here, for readability, we absorb this factor  $\mu$  into  $\lambda^{(0)}$ .
- [31] W. Wang, M. Tang, H. E. Stanley, and L. A. Braunstein, Unification of theoretical approaches for epidemic spreading on complex networks, *Rep. Prog. Phys.* **80**, 036603 (2017).
- [32] L. Bremaud, O. Giraud, and D. Ullmo, Analytical solution of susceptible-infected-recovered models on homogeneous networks, *Phys. Rev. E* **110**, 044307 (2024).
- [33] L. Bremaud, Mean field game description of virus propagation, Ph.D. thesis, Université Paris-Saclay, 2024.
- [34] All the data used for the simulations in this manuscript are openly available, see [38].
- [35] S. Eubank, H. Guclu, V. Anil Kumar, M. V. Marathe, A. Srinivasan, Z. Toroczkai, and N. Wang, Modelling disease outbreaks in realistic urban social networks, *Nature (London)* **429**, 180 (2004).
- [36] G. Béraud, S. Kazmerczak, P. Beutels, D. Levy-Bruhl, X. Lenne, N. Mielcarek, Y. Yazdanpanah, P.-Y. Boëlle, N. Hens, and B. Dervaux, The French connection: The first large population-based contact survey in France relevant for the spread of infectious diseases, *PLoS ONE* **10**, e0133203 (2015).
- [37] L. Di Lucchio and G. Modanese, Generation of scale-free assortative networks via Newman rewiring for simulation of diffusion phenomena, *Stats* **7**, 220 (2024).
- [38] L. Bremaud, D. Ullmo, and O. Giraud, Parameters for epidemic simulations on heterogeneous networks (1.0) [Data set], Zenodo (2025), doi:[10.5281/zenodo.17220446](https://doi.org/10.5281/zenodo.17220446).